Neuroprotective potential of solanesol in a combined model of intracerebral and intraventricular hemorrhage in rats

Kajal Rajdev, Ehraz Mehmood Siddiqui, Kuldeep Singh Jadaun, Sidharth Mehan*

Neuropharmacology Division, ISF College of Pharmacy, Moga, 142001 Punjab, India

ABSTRACT

Intracerebral hemorrhage (ICH) may be caused by trauma, aneurysm and arteriovenous malformation, as can any bleeding within the intracranial vault, including brain parenchyma and adjacent meningeal spaces (aneurism and atreovenous malformation). ICH is the cerebral stroke with the least treatable form. Over time, intraventricular hemorrhage (IVH) is associated with ICH, which contributes to hydrocephalus, and the major cause of most hemorrhagic death (Due to the cerebral hemorrhage and post hemorrhagic surgeries). Most patients suffer from memory impairment, grip strength, posture, and cognitive dysfunctions attributable to cerebral hemorrhage or post-brain hemorrhagic surgery. Nevertheless, a combined model of ICH based IVH is not present pre-clinically. Autologous blood (ALB) injection (20 μl/5 min) in the rat brain triggers hemorrhage, such as factors that further interfere with the normal functioning of neuroinflammatory cytokines, oxidative stress, and neurotransmitter dysfunction, such as CoQ10 insufficiency and dysregulation of mitochondrial ETC-complexes. For the prevention of post-brain hemorrhagic behavioral and neurochemical dysfunctions, there is no specific drug treatment available, only available therapy used to provide symptomatic relief. The current study reveals that long-term administration of Solanesol (SNL) 40 and 60 mg/kg alone and in combination with available drug therapy Donepezil (DNP) 3 mg/kg, Memantine (MEM) 20 mg/kg, Celecoxib (CLB) 20 mg/kg, Pregabalin (PGB) 30 mg/kg, may provide the neuroprotective effect by improving behavioral and neurochemical deficits, and gross pathological changes in ALB induced combined experimental model of ICH-IVH in post brain hemorrhagic conditions in rats. Thus, SNL can be a potential therapeutic approach to improve neuronal mitochondrial dysfunction associated with post brain hemorrhagic behavioral and neurochemical alterations.

1. Introduction

Intracerebral hemorrhage (ICH) can be defined as any intracranial vault bleeding, including the brain parenchyma and surrounding meningeal spaces (Caceres and Goldstein, 2012). IVH is a condition in which blood leaks into the intracranial vault leading to hematoma formation (Caceres and Goldstein, 2012) that further damages the ventricles leading to cerebrospinal fluid leakage which cumulatively causes symptoms such as sudden tingling, weakness, numbness, paralysis, severe headache, difficulty swallowing or vision, loss of balance or vision coordination, difficulty understanding, speaking reading or writing and a change in level of consciousness and alertness marked by stupor, lethargy, sleepiness or coma. Bleeding directly into the ventricles from a source or lesion is in contact with or part of a ventricular wall as intraventricular hemorrhage (IVH) is known as a vascular malformation (Findlay, 2011). The signs and symptoms include multiple cognitive, emotional and physical impairments, such as aphasia,

gaze deviation hemianopia, hyperactive tendon jerks, muscle stiffness, thus interfering with regular movements, voice and gait impacting social quality of life, and the ability to work in brain hemorrhagic patients (Nedergaard et al., 1983; Wityk and Caplan, 1992; Wallmark et al., 2014; Marinkovic and Tatlisumak, 2014). (ICH is the least treatable form of stroke and associated with the worst prognosis in up to 40 % of cases, ICH further complicated by IVH which leads to condition hydrocephalus and increases case mortality up to 80 %. Depending on the underlying cause of bleeding ICH is classified as either primary or secondary Primary ICH, which accounts for 78–88% of cases, is caused by the spontaneous rupture of small vessels weakened by chronic hypertension or amyloid angiopathy (Aronowski and Hall, 2005). Secondary ICH occurs in combination with trauma, vascular abnormalities, tumors or coagulation impaired (Qureshi et al., 2001).

There are currently no specific FDA-approved post-brain hemorrhage therapy medications to enhance functional outcomes in ICH patients due to their various injury mechanisms (Fiorella et al., 2015).

Primary ICH contributes to blood leakage in the brain parenchyma and further raises intracranial pressure that is responsible for killing neurons and glial cells (Xi and Keep, 2012). Various preclinical studies show that secondary brain injury following ICH is caused by cytotoxicity interactions (Hu et al., 2016), excitotoxicity, oxidative stress, inflammation, and mitochondrial dysfunction (Aronowski and Zhao, 2011) from red blood cell lysis products and plasma component accumulation (Chaudhary et al., 2013). However, it remains to be thoroughly elucidated the exact pathophysiological processes underlying ICH. (Elevation in intracranial pressure and acute vasoconstriction are two major factors responsible for reduced cerebral blood flow responsible for ischemic conditions. Initial hematoma induces glutamate release and then leads to oxidative stress and mitochondrial dysfunction). The most important implications for ICH pathogenesis are oxidative stress and neuronal cell damage associated with cognitive decline (Gong et al., 2001; Kim et al., 2017).

In the delayed phase of ICH, pathologically released noxious protease substances such as matrix metalloproteinase (MMP-9) from neutrophils, and activated microglia cause structural damage to the blood-brain barrier (BBB) leading to brain swelling (Turner and Sharp, 2016). The release of erythrocyte lysis products such as iron which catalyzes the development of free radicals and reactive oxygen species (ROS) is the main mediator of the inflammatory cascade which leads to cell death and perihematomal swelling. Mitochondrial dysfunction contributes significantly to the deficiency of the results produced by adenosine triphosphate (ATP) in the failure of cellular ion pumps causing cytotoxic swelling and neuronal apoptosis (Sook Kim-Han et al., 2006) (Hence, neuroprotection in ICH needs a combined approach of decreasing different byproducts of secondary brain damage such as oxidative stress and mitochondrial dysfunction and restoring the antioxidant mechanism in the brain).

Specific ICH experimental animal models are used to research ICH pathophysiology and pharmacological interventions (including the micro balloon model (Sinar et al., 1987), the bacterial collagenase injection model (Lu et al., 2015) and the autologous blood (ALB) injection model (Strbian et al., 2007., Sinar et al., 1987; Lu et al., 2015; Strbian et al., 2007). We tried to use a low volume of autologous blood to minimize the mortality rate. Because the combined ICH and IVH model has high mortality due to the use of a large volume of autologous blood. For this, in the current study, we injected low volume (20 microliters) of autologous blood into the rat brain to ensure the presence of blood in both brain parenchyma and ventricles and low mortality rates (5.4 %) compared to other brain hemorrhagic studies (Strbian et al., 2007; Marinkovic and Tatlisumak, 2014, Marinkovic and Strbian, 2014). Intracerebroventricular (ICV) administration of autologous blood (ALB) has been shown to induce marked neurological deficits and neuronal cell damage in experimental rats. In the combined ALB injection model, the hematoma size is controllable, which depends on the amount of blood injected. This blood model mimics a single large bleed that is thought to occur in most ICH patients and is most commonly used to investigate mechanisms of hemorrhagic damage in experimental rats.

In addition, combined autologous blood (ALB) injection into the brain of rats triggers hemorrhage as a disease that further interferes with the normal functioning of neuronal mitochondria such as CoQ10 insufficiency and ETC-complex dysregulation (Kim-Han et al., 2006), which is also responsible for neuropathological cascades such as increases neuroinflammatory cytokines (Brunswick et al., 2012), oxidative stress (Duan et al., 2016), neurotransmitter imbalance, (Prentice et al., 2015) failure of cellular pumps causing cytotoxic swelling and neuronal apoptosis. Nonetheless, in the prevention of post-brain hemorrhagic behavioral and neurochemical changes, there is no specific drug treatment available and only effective drug therapy is required to provide symptomatic relief like donepezil (DNP) (Masanic et al., 2001), memantine (MEM) (Kafi et al., 2014), celecoxib (CLB) (Park et al., 2009), and pregabalin (PGB) (Rahajeng et al., 2018).

To restore the neuronal integrity and prevent neurological deficits

solanesol (SNL) as a coenzyme Q10 (CoQ10) precursor is used in the current study (Mehan et al., 2018). Solanesol is a 45 carbon isoprenoid isolated from tobacco leaves (Tang et al., 2007) (*Nicotiana tobacum*), tomato (*Solanum lycopersicum*) (Arab et al., 2019), potato (*Solanum tuberosum*) (Campbell et al., 2016), eggplant (*Solanum melongena*) and pepper (*Solanum melongena*) (Kotipalli et al., 2008) (Tobacco has the highest SNL content among all the solanaceous plant). SNL is the starting medium for the synthesis of ethylenediamine (SDB) CoQ9, coenzyme Q10, vitamin-K2, vitamin-E and N-solanesyl-N, N′-bis-(3,4-dimethoxybenzyl) (Campbell et al., 2016). It is commonly used as a crucial intermediate for the synthesis of ubiquinone drugs in the pharmaceutical industry (e.g., CoQ10) (Zhao et al., 2006).

SNL is a precursor of CoQ10 and a powerful antioxidant with anti-inflammatory properties and membrane stability (Guo et al., 2008; Qin et al., 2017). Because, CoQ10 is an essential co-factor in the respiratory chain of the mitochondria and can restore the loss of mitochondrial transmembrane capacity, resulting in reduced mitochondrial ROS production and thus protecting the mitochondria and cellular components from oxidative damage.

CoQ10 (2, 3 dimethoxy-5-methyl-6-decaprenyl benzoquinone) is the most common coenzyme of 10 repeated isoprene units in human mitochondria, also known as ubiquinone (Turunen et al., 2000; Barcelos and Haas, 2019). CoQ10 is a part of the electron transport chain that receives electrons from complex-I and pumps protons across the inner mitochondrial membrane and moves the electrons to complex-II, which is also responsible for ATP production (Orsucci et al., 2011; DeLegge and Smoke, 2008) and will reduce oxidative neuron damage and enhance animal behavior. (Mehan et al., 2018). CoQ10 has documented potential for treating Autism (Sharma et al., 2019), migraine (Sa´ndor et al., 2005), Huntington's disease (Mehan et al., 2018), and other neurodegenerative diseases such as Parkinson's disease, Amyotrophic lateral sclerosis, Alzheimer's disease, and multiple sclerosis (Matthews et al., 1998; Shults et al., 2004). The present study, therefore, investigated the potential of solanesol alone and in combination with approachable therapy against the combined intracerebral and intraventricular hemorrhage model induced by autologous blood injection.

2. Material and methods

2.1. Experimental animals

Adult Wistar rats ($250 - 300$ g, total animal = 54, 30 male and 24 female) obtained free access to food and water from the Central Animal House facility of ISF College of Pharmacy, Moga, Punjab (India) (The total number of animals housed under a 12-h light/12-h dark cycle for at least 1 week before the start of the experiment in polyacrylic cages (three rats per cage) with free access to food and water). All behavioral parameters were tested from 9:00 am to 17:00 h. The study protocol approved by the Institutional Animal Ethics Committee (IAEC / CPCSEA / M 23/372) and experiments conducted under the guidelines of the Indian National Science Academy (INSA) for the use and care of experimental animals.

2.2. Drugs and chemicals

The test drugs Solanesol (SNL), Pregabalin (PGB), Celecoxib (CLB), Memantine (MEM), and Donepezil (DNP) were procured from BAPEX Pharmaceuticals, India as *ex-gratia* samples. Heparin sodium injection (1000 USP units per ml; Baxter Healthcare Corporation). Sterile alcohol preparation pads (Phoenix Healthcare Solutions), sterile saline solution (0.9 % (wt/vol) NaCl in distilled water). Neomycin (10 g; GSK), Gentamycin (80 mg; Intogen), Lignocaine gel (Lox 2% Jelly; Neon Laboratories Limited), Sodium pentobarbital (Sanofi Aventis, India). SNL dissolved in water with 2% ethanol administered by the oral route *(p.o.)*. PGB 30 mg/kg (Song and Jun, 2017), CLB 20 mg/kg (Sinn and
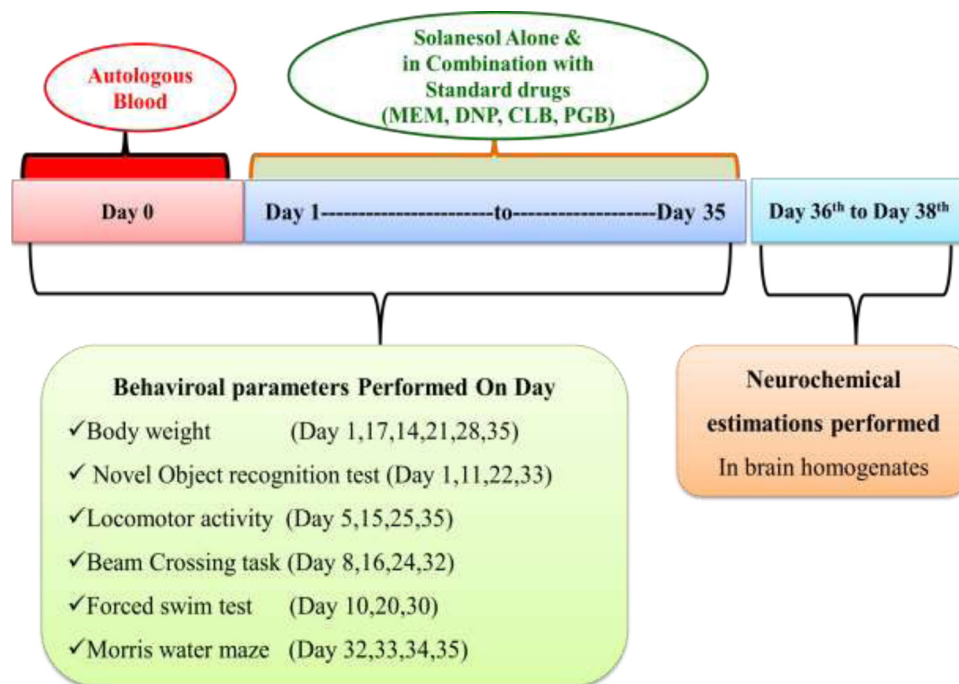
Fig. 1. Experimental protocol schedule (Behavioral and biochemical estimations).

Lee, 2007), MEM 20 mg/kg (Lee and Chu, 2006), and DNP 3 mg/kg (Zhang and Plotkin, 2004) dissolved in saline and administered by intraperitoneally (i.p.). All other chemicals used in the study are of analytical grade. Solutions of the drugs and chemicals freshly prepared before use.

2.3. Experimental protocol schedule

The total duration of the study was 35 days (Gao et al., 2014). On day 0 autologous blood (ALB) was administered intracerebroventricularly. SNL chronically administered from day 1 after ALB administration until the end of the study (the 35th day) (Fig. 1). Dose selection was done according to previous studies (Mehan et al., 2018). Treatment with standard drugs such as CLB, MEM, PGB, and DNP also started from day one of the studies. Animals randomly assigned to 9 groups (n = 6 for each group). Group 1 Sham Control, Group 2 Solanesol perse (60 mg/kg, p.o.), Group 3- ALB (20 μl, i.c.v.), Group 4 ALB (20 μl, i.c.v.) + SNL (40 mg/kg, p.o.), Group 5 ALB (20 μl, i.c.v.) + SNL (60 mg/kg, p.o) Group 6 ALB (20 μl, i.c.v.) + SNL (60 mg/kg, p.o) + MEM (20 mg/kg, i.p.), Group 7 ALB (20 μl, i.c.v.) + SNL (60 mg/kg, p.o) + PGB (30 mg/kg, i.p.), Group 8 ALB (20 μl, i.c.v.) + SNL (60 mg/kg, p.o) + DNP (3 mg/kg, i.p.), Group 9 ALB (20 μl, i.c.v.) + SNL (60 mg/kg, p.o) + CLB (20 mg/kg, i.p.). Various behavioral assessments were carried out from day 1 to day 35. On day 36, the animals were deeply anesthetized with sodium pentobarbital (270 mg/mL, i.p.) and transcardially perfused with ice-cold PBS (0.1 M) followed by 4% paraformaldehyde in PBS for biochemical analysis of the brain. The experimental protocol summarized in (Fig. 1).

2.4. Combined model of ICH-IVH in experimental animals

Wistar rats were anesthetized using ketamine (75 mg/kg, i.p.) (Rynkowski and Kim, 2008) and placed in a stereotactic frame. The head was shaved and a midline scalp incision was made to expose the skull, and a burr hole was made to introduce a calibrated hamilton syringe into the cerebroventricular part of the brain (stereotaxic co-ordinates from bregma: 0.26 mm antero-posterior, 2.2 mm medio-lateral, 5.0 mm dorso-ventral). The withdrawal site was disinfected with

70 % alcohol pads. Twenty five-G needle into the vein was inserted and a capillary tube was used to collect the blood. Twenty microlitres of ALB withdrawn from the central tail artery or lateral tail veins (Marinkovic and Tatlisumak, 2014). Polyethylene tubing connected to the end of the hamilton syringe and filled with heparin where, 2 microlitres of air drawn into this tubing, followed by two microlitres of saline (Rynkowski and Kim, 2008). This was done to leave a small air bubble between saline and heparin to prevent the mixing of these reagents. Again, 2 microlitres of air were drawn into the tubing followed by 20 microlitres of previously collected blood. Twenty microlitres of autologous blood were injected over 5 min (Xue and Del Bigio, 2000). The burr hole filled with dental cement and fixative after completion of the infusion and the skin was sutured. 'Immediately post-surgery all rats received the subcutaneous injection of analgesic (ketoprofen, 1 mL/kg) and antibiotic gentamycin (35 mg/kg, i.p) was given twice a day of 12 h to prevent infection. Lignocaine and neomycin applied topically to prevent pain and infection, respectively. Animals were fed with oral glucose for 4 days along with a normal chow diet following surgery and then replaced with normal water and chow diet. Body weight was measured on days 1, 7, 14, 21, 28and 35 days of the experiment.

2.5. Parameters evaluated

2.5.1. Behavioral parameters
2.5.1.1. Morris water maze. The Morris water maze (MWM) was utilized to assess cognitive function by measuring escape latency on day 32, 33, 34, 35 and time spent in the target quadrant (TSTQ) recorded on day 35. The protocol was designed as described by Qin et al. (2018). (In the reference memory test, a platform was placed in the southwest quadrant 2 cm below water. Each animal was given 4 trials per day i.e. before day 0, starting from one of the release points in different directions. The inter-trial interval was 15 min). The working memory was executed on day thirty seconds after induction of hemorrhage, and escape latency was recorded. Each trial of the reference and working memory tests were ended when the rat stationed on the platform for 10 s or 120 s had elapsed. (The rats would be guided to stand on the platform if they did not find it within 120 s, and then the escape latency was recorded as 120 s.) On day 35,

the rats were subjected to the probe trial, in which the platform was removed and TSTQ was recorded. All the data was recorded and analyzed by video tracking.

2.5.1.2. Forced swim test. On days 10, 20 and 30 post-ICH-IVH, each rat underwent the forced swim test (FST) based on an established protocol with minor modifications (Roh et al., 2016). Rats were placed individually in cylindrical tanks (height, 50 cm; diameter, 15 cm) containing 30 cm of water at 24 ± 1 ˚C. A camera recorded the movement of the rat for 5 min. (All the experimental rats underwent a pretest for 15 min to eliminate the acute stress of the water and to provide the animals with the ability to adapt to the water. Twenty-four hours after the pretest, the animals were tested for 5 min.). The immobility time was calculated by subtracting the total amount of mobility time over the 5 min of testing. The rat was judged to be immobile when it ceased struggling and remained floating motionless in an upright position in the water, making only small movements to keep its head above the water (Zhu et al., 2014).

2.5.1.3. Beam crossing task. The beam-walking test (1.0 cm diameter, 80 cm long beam) was performed to evaluate hind limb dysfunction on days 8, 16, 24 and 32 after surgery. The function of the right paralyzed hind limb was evaluated. Performance rated on a 7 point scale: (1) the rat was unable to place the affected hind limb on the horizontal surface of the beam; (2) the rat places the limb on the beam and maintains balance but unable to traverse the beam; (3) the rat traverses the beam dragging the affected hind limb; (4) the rat traverses the beam and places the affected hind limb on the horizontal surface of the beam once; (5) the rat crosses the beam and places the affected hind limb on the horizontal surface of the beam to aid during less than half of the steps; (6) the rat uses the affected hind limb to aid in more than half of the steps; and (7) the rat traverses the beam with only two-foot slips (Takamatsu et al., 2016).

2.5.1.4. Locomotor activity. Locomotor activity was monitored on days 5, 15, 25 and 35 using an actophotometer (IMCORP, Ambala, India). (The motor activity in the actophotometer detected by photocells installed in the instrument). Animals were placed individually in the activity chamber for 3 min as a habituation period before making an actual recording. Each animal was observed over 5 min and expressed as counts per 5 min (Singh et al., 2017).

2.5.1.5. Novel object recognition test. On days 1, 11, 22 and 33post-ICH, an established protocol was used to test each rat in the novel object recognition test. (On the first day, the rat was placed in a cage and habituated to explore an open field for 5 min. On the second day, two identical novel objects (wooden brown cubes) were placed in the arena, and the rat was allowed to explore them for 10 min. After 1 h, the rat was given one novel object (white ball, 5 cm in diameter) and one familiar one (wooden brown cube) and allowed to explore for 5 min). A camera recorded the behaviors displayed by each rat during the test. We compared the total time spent exploring new and old objects. Time spent exploring an object included time in direct contact and time within the object area. The rat was considered in the object area if its nose was directed at the object and less than approximately two centimeters from it (Zhu et al., 2014).

2.6. Mitochondrial ETC-complexes enzyme activity

2.6.1. Isolation of rat brain mitochondria

Rat brain mitochondria were isolated using Berman and Hastings, 1999 method for mitochondrial enzyme complex activities. Isolated brains were homogenized, and homogenates then centrifuged at $13,000 \times g$ for 5 min at 4 ˚C. Pellets were re-suspended in isolation buffer with ethylene glycol tetra-acetic acid (EGTA) and spun again at $13,000 \times g$ at 4 ˚C for 5 min. The resulting supernatants were transferred

to new tubes and topped off with isolation buffer with EGTA and again spun at $13,000 \times g$ at 4 ˚C for 10 min. Pellets containing pure mitochondria were resuspended in isolation buffer without EGTA. (Bhardwaj and Kumar, 2016)

2.6.2. Mitochondrial nicotinamide adenine dinucleotide dehydrogenase (NADH) (Complex-I) enzyme activity

King and Howard (1967a) method were used for the measurement of NADH dehydrogenase activity spectrophotometrically. (The method involves catalytic oxidation of NADH to NAD^+ with subsequent reduction of cytochrome C. The reaction mixture contained 0.2 M glycylglycine buffer (pH 8.5), 6 mM NADH in 2 mM glycylglycine buffer, and 10.5 mM cytochrome C.) The reaction was initiated by the addition of a requisite amount of solubilized mitochondrial sample followed by an absorbance change at 550 nm for 2 min. The values expressed as nM/mg protein.

2.6.3. Succinate dehydrogenase (SDH) (complex-II) activity

SDH measured spectrophotometrically using the method by King, 1967b). The method involves the oxidation of succinate by an artificial electron acceptor, potassium ferricyanide. (The reaction mixture contained 0.2 M phosphate buffer (pH 7.8), 1% BSA, 0.6 M succinic acid, and 0.03 M potassium ferricyanide.) The reaction initiated by the addition of the mitochondrial sample followed by an absorbance change at 420 nm for 2 min. The values expressed as nM/mg protein.

2.6.4. Complex-V activity (ATPase)

ATP synthase Enzyme Activity Microplate Assay Kit ab109714 was used to determine the activity of ATP synthase (Complex-V). (The ATP synthase enzyme was immunocaptured within the wells of the microplate and the enzyme activity measured by monitoring the decrease in absorbance at 340 nm). The conversion of ATP to ADP by ATP synthase is coupled to the oxidation reaction of NADH to NAD^+ with a reduction in absorbance at 340 nm. The values expressed as nM/mg protein (Kanamoto et al., 2019).

2.6.5. Mitochondrial ETC-complex CoQ_{10} level

CoQ10 from brain tissues and mitochondria was extracted and measured by HPLC as described by Okamoto et al. (1985). Briefly, tissue or mitochondria were homogenized using a micro-glass tissue grinder in 0.5 mL potassium phosphate buffer pH 7.4 containing 1 mM dithiothreitol. The homogenate was treated with 2 mL of ethanol containing 1 μg/mL butylated hydroxytoluene (Sigma, St. Louis, MO) and ubiquinone was extracted with 5 mL hexane. After vigorous shaking, 4 mL of the hexane layer dried under N_2. The residue dissolved in a hundred μl ethanol containing BHT and subjected to HPLC analysis. CoQ_9 and CoQ_{10} quantified using the C_{18} column with a mobile phase methanol: hexane (90:10 v/v), detected at a wavelength of 275 nm. The values expressed as nM/mg protein.

2.6.6. Assessment of neurotransmitter level

2.6.6.1. Measurement of GABA and glutamate levels. The GABA and glutamate levels were estimated by the method described by Donzanti (Donzanti and Yamamoto, 1988) with slight modifications, which involved HPLC with an ECD. (A Waters standard system comprising a high-pressure isocratic pump, a 20 microlitres manual sample injector valve, a C_{18} reversed-phase column, and an ECD used in the study. The mobile phase comprised 100 mM anhydrous disodium hydrogen phosphate, 25 mM EDTA, and 22 % methanol (pH: 6.5). The electrochemical conditions for the experiment were +0.65 V, with sensitivity ranging from 5 to 50 nA. The separation was carried out at a flow rate of 1.2 mL/minutes, and the column temperature maintained at 40 ˚C. Samples (20 μl) injected manually through a rheodyne valve injector. On the day of the experiment, the frozen brain samples thawed and homogenized in 0.2 M perchloric acid. Then, the samples anteroposterior at $12,000 \times g$ for 15 min. The supernatant was

derivatized using OPA/β-ME (o-pthalaldehyde/β-mercaptoethanol) and then filtered through the 0.22-mm nylon filters before being injected into the HPLC sample injector). Data were recorded and analyzed using Breeze software version 3.2 purchase from Waters HPLC. The amino acid concentrations calculated from the standard curve generated using a standard in the concentration range of 10–100 ng/ml. The values expressed as a percentage of the normal control group.

2.6.6.2. Estimation of dopamine level. The levels of dopamine in the brain were estimated via high-performance liquid chromatography (HPLC) using an electrochemical detector (ECD) (Jamwal and Kumar, 2016). A Waters standard system comprising a high-pressure isocratic pump, a 20 microlitres manual sample injector valve, a C_{18} reversed-phase column, and an ECD used in the study. The mobile phase comprised of sodium citrate buffer (pH 4.5)–acetonitrile (87:13, v/v). The sodium citrate buffer comprised 10 mM citric acid, 25 mM NaH_2PO_4, 25 mM EDTA (ethylene diamine tetra-acetic acid), and 2 mM 1-heptane sulfonic acid. The electrochemical conditions for the experiment were +0.75 V, with sensitivity ranging from 5 to 50 nA. The separation carried out at a flow rate of 0.8 mL/minutes. The samples (20 microlitres) were injected manually. On the day of the experiment, the frozen brain samples thawed and homogenized in a homogenizing solution containing 0.2 M perchloric acid. Then, the samples were centrifuged at $12,000 \times g$ for 5 min. The supernatant filtered through 0.22-mm nylon filters before being injected into the HPLC sample injector). Data were recorded and analyzed with Breeze software.

2.6.6.3. Estimation of acetylcholine (Ach). A diagnostic kit (Krishgen diagnostics, India) was used to measure acetylcholine. Samples and all the reagents were prepared as described in the kit. The optical density of the reaction mixture was determined at 540 nm in the microtiter plate (Zeng et al. 2017).

2.6.7. Estimation of neuroinflammatory biomarkers
2.6.7.1. Estimation of TNF-α, IL-1β, IL-10 levels. A diagnostic kit (Krishgen diagnostics, India) was used to measure TNF-α, IL-1β, IL-10. Samples and all the reagents were prepared as described in the kit. The optical density of the reaction mixture determined at 450 nm in the microtiter plate (Wang et al., 2018).

2.6.8. Protein estimation
The protein content was measured using the coral protein estimation kit using the biuret method (Gornall et al., 1949).

2.6.9. Assessment of oxidative stress markers
2.6.9.1. Preparation of rat brain homogenate. On day 36, animals were sacrificed by decapitation; brains were removed and rinsed with ice-cold isotonic saline solution. Brain samples then homogenized with a chilled phosphate buffer 0.1 M phosphate buffer (7.4). The homogenate centrifuged at $10,500 \times g$ for 15 min, supernatant separated and aliquots used for biochemical estimation (Hussein et al., 2012).

2.6.9.2. Measurement of acetylcholinesterase (AChE) levels. The quantitative measurement of acetylcholinesterase activity in the brain was performed according to the method described by Ellman (Ellman et al., 1961). (The assay mixture contained 0.05 mL of supernatant, 3 mL of 0.01 M sodium phosphate buffer (pH 8), 0.10 mL of acetyl thiocholine iodide and 0.10 mL of DTNB (Ellman reagent).) The change in absorbance measured immediately at 412 nm spectrophotometrically. The enzymatic activity in the supernatant expressed as μmol/mg protein.

2.6.9.3. Estimation of reduced glutathione levels. Levels of glutathione in the brain were estimated according to the method described by Ellman (Ellman, 1959). One ml supernatant precipitated with 1 mL of 4%

sulfosalicylic acid and cold digested at 4 °C for 1 h. The samples centrifuged at $1200 \times g$ for 15 min. To 1 mL of the supernatant, 2.7 mL of phosphate buffer (0.1 M, pH 8) and 0.2 mL of 5,5′-dithiobis-(2-nitrobenzoic acid) (DTNB) were added. The yellow color that developed was measured immediately at 412 nm using a spectrophotometer. The concentration of glutathione in the supernatant expressed as μM/mg protein (Singh et al., 2017).

2.6.9.4. Assessment of malondialdehyde (MDA) levels. The quantitative measurement of malondialdehyde (MDA) end product of lipid peroxidation–in brain homogenate was performed according to the method of Wills (1966). The amount of MDA was measured, after its reaction with thiobarbituric acid, at 532 nm using a spectrophotometer (PERKIN ELMER UV/VIS Spectrophotometer, Lamda 20). The concentration of MDA expressed as nM/mg protein (Cai et al., 2015).

2.6.9.5. Assessment of superoxide dismutase (SOD) activity. The SOD activity assayed using the method described by Kono (1978). The assay system comprises 0.1 mmol/L EDTA, 50 mmol/L sodium carbonate and 96 mmol/L of nitro blue tetrazolium. In the cuvette, 2 mL of the above mixture, 0.05 mL of hydroxylamine and 0.05 mL of the supernatant added and auto-oxidation of hydroxylamine measured for two minutes at 30′s interval by measuring the absorbance at 560 nm (PERKIN ELMER UV/VIS Spectrophotometer, Lamda 20). The activity of SOD expressed as units/mg protein (Cai et al., 2015).

2.6.9.6. Estimation of nitrite levels. The accumulation of nitrite in the supernatant, an indicator of the production of nitric oxide (NO), determined by a colorimetric assay using Greiss reagent (0.1 % N-(1-naphthyl) ethylenediamine dihydrochloride, 1% sulfanilamide and 2.5 % phosphoric acid) as described by Green et al. (1982). Equal volumes of supernatant and Greiss reagent mixed, the mixture incubated for ten minutes at room temperature in the dark and the absorbance determined at 540 nm spectrophotometrically. The concentration of nitrite in the supernatant was determined from the sodium nitrite standard curve and expressed as μg/mL proteins (Singh et al., 2017).

2.6.9.7. Gross pathological examination and measurement of hematoma size of rat brain. Animals were sacrificed by decapitation on day 36; brains were removed for gross pathological analysis. Coronal sections were taken after observation of the whole rat brain. (Liu et al., 2015). For the measurement of hematoma size, the brain was removed quickly, submerged for 1 min in ice-cold saline, and placed on a tissue chopper to determine the volume of the hematoma. Sectioned 2-mm thick brain pieces (coronally from the anterior pole to the posterior poles of the cerebral cortex) were placed on glass slides. A digital camera (Fujix digital camera, Fujifilm, Japan) was used to view all the parts of the brain that span the whole striatum. This took less than 5 min to take digital images of all brain parts including a hematoma in each brain section. The collected digital images were processed for the preparation of figures and converted to TIFF files for image analysis. The hematoma region (mm) in each brain segment was measured on day 36th after completion of the procedure through MOTICAM-BA310 image plus 2.0 analysis software. The volume of the hematoma scale (mm^3) was measured for each coronal brain segment by conversion of the hematoma region (mm) (Terai et al., 2003).

The hematoma size (mm^3) in each brain section was determined from the red area in the striatum by image analysis on the 36th day, after induction of ICH. The size of the hematoma was calculated in each coronal 2-mm-thick brain section by calculating the hematoma area (lXbxh).

2.7. Statistical analysis

Graph Pad Prism (Graph Pad Software, San Diego, CA, USA) used for all statistical analyses. Values expressed as mean ± SEM. The
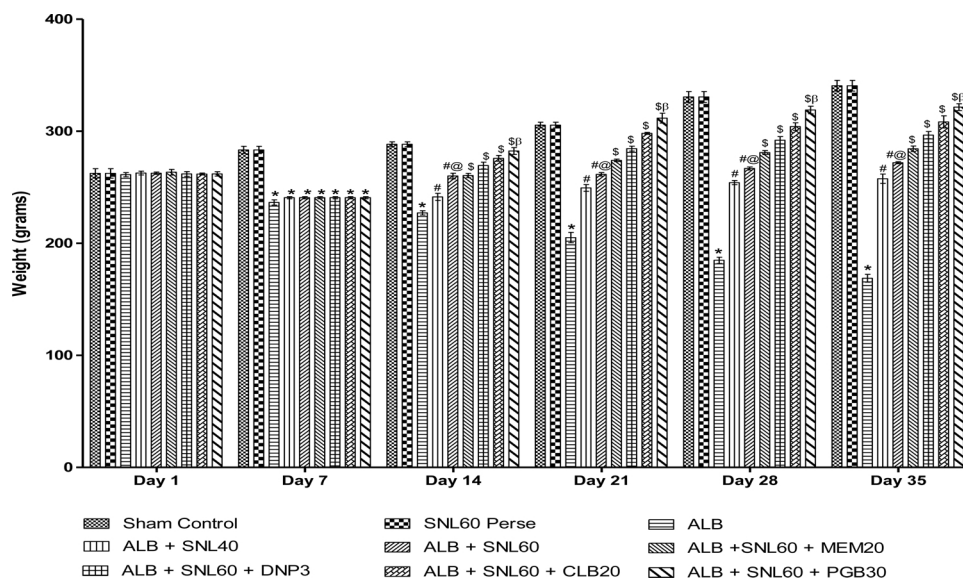
behavioral assessment data analyzed by two-way analysis of variance (ANOVA) with drug-treated groups as between sessions and as within-subjects factors. The biochemical estimations analyzed by one-way ANOVA. Post hoc comparisons between groups were made using Tukey's post hoc test. p < 0.001 was considered significant.

3. Results

3.1. Neuroprotective effect of SNL on body weight in ALB induced brain hemorrhagic rats

Treatment with ALB induced a significant reduction in body weight compared to normal rats. Treatment with SNL 60 mg/kg perse showed no change in body weight over normal rats. Post-treatment with continuous administration of SNL 40 mg/kg and SNL 60 mg/kg successfully reversed the loss of body weight caused by ALB as compared to normal and 60 mg/kg perse. Treatment with SNL 60 mg / kg in combination with PGB 30 mg / kg has substantially and dose-dependently restored body weight relative to other standard drug treatment groups CLB 20 mg / kg, DNP 3 mg / kg, and MEM 20 mg / kg in the combined ICH-IVH rat model (p < 0.001) (Fig. 2).

3.2. Behavioral parameters

3.2.1. Neuroprotective effect of SNL on spatial navigation task in ALB induced brain hemorrhagic rats using morris water maze

During the reference memory test, the escape latency of the trained rats in the Morris water maze test gradually reduced. ALB induced ICH-IVH in rats increased the escape latency time on day 32, 33, 34, and 35 when compared to the normal group (p < 0.001). Treatment with SNL 60 mg/kg perse did not show any difference in escape latency compared to normal rats. After hemorrhage, chronic treatment with SNL 40 mg/kg, and SNL 60 mg/kg decrease the latency time. Treatment with SNL 60 combined with DNP 3 substantially and dose-dependently increased the escape latency compared to SNL 60 in combination with MEM 20 mg/kg, PGB 30 mg/kg and CLB 20 mg/kg (p < 0.001). On day 35, TSTQ was decreased in ALB mediated ICH-IVH rats compared to normal and SNL 60 mg/kg perse treated rats. Post-treatment with SNL 40 mg / kg and SNL 60 mg / kg considerably improved the TSTQ. Treatment with SNL 60 mg / kg combined with DNP 3 mg / kg significantly improved the duration of the escape latency compared to SNL 60 in combination with MEM 20 mg / kg, PGB 30 mg / kg and CLB 20 mg/kg (p < 0.001) (Figs. 3 and 4).

3.2.2. Neuroprotective effect of SNL on immobility using forced swim test in ALB induced brain hemorrhagic rats

ALB induced ICH-IVH in rats, showing the depression-like activity increased immobility time in FST. Groups with only autologous blood, compared to normal rats, showed a significant increase in immobility time. Chronic SNL 60 mg/kg perse treatment showed no depression-like activity as compared to normal rats. Consequently, post-treatment with SNL 40 mg / kg and SNL 60 mg / kg for 35 days decreased the immobility time compared to normal and SNL 60 mg / kg per se. SNL 60 treatment in combination with PGB 30 mg / kg prodigiously improved immobility compared to SNL 60 mg / kg in combination with CLB 20 mg / kg, MEM 20 mg / kg and DNP 3 mg / kg (p < 0.001) (Fig. 5).

3.2.3. Neuroprotective effect of SNL on the neurological score using beam crossing task in ALB induced brain hemorrhagic rats

During beam crossing activity, ICH-IVH rats induced ALB exhibited greater dysfunction of the hind limbs compared with normal rats. Compared to normal animals, single autologous blood groups showed a significant decrease in neurological scores SNL 60 mg/kg perse treatment showed no motor dysfunction when compared with normal rats. Post-treatment with SNL 40 mg / kg and SNL 60 mg / kg over 35 days considerably improved the neurological performance. Treatment with SNL 60 mg / kg in combination with CLB 20 mg / kg significantly and dose-dependently improved the neurological score compared to SNL 60 mg / kg in combination with PGB 30 mg / kg, MEM 20 mg / kg, and DNP 3 mg / kg (p < 0.001) (Fig. 6).

3.2.4. Neuroprotective effect of SNL on locomotor activity using actophotometer in ALB induced brain hemorrhagic rats

In rats, ALB induced ICH-IVH caused a significant decline in locomotive activity as compared to normal rats. Chronic SNL 60 mg/kg perse treatment showed no improvement in locomotive behavior as compared with normal rats. Post-treatment with SNL 40 mg/kg and SNL 60 mg/kg during 35 days improved the locomotive activity significantly. Treatment with SNL 60 mg / kg in combination with PGB 30 mg / kg significantly improved the locomotion compared with SNL 60 mg / kg in combination with CLB 20 mg / kg, MEM 20 mg / kg and DNP 3 mg / kg (p < 0.001) (Fig. 7).

3.2.5. Neuroprotective effect of SNL on exploration time using novel object recognition task in ALB induced brain hemorrhagic rats

In the novel object recognition test, ALB induced ICH-IVH in rats with impaired memory as compared to normal rats and confirmed
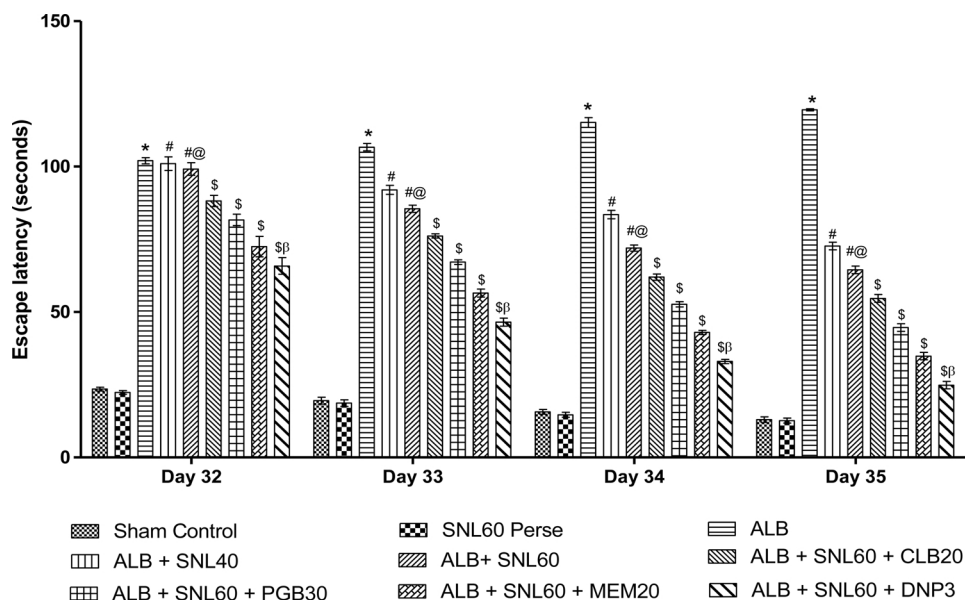
Fig. 3. Neuroprotective effect of SNL on escape latency in ALB induced ICH-IVH in rats using morris water maze.
Data expressed as mean ± SEM (n = 6). * p < 0.001 versus sham control and SNL60 *perse*; # p < 0.001 versus ALB; #@ p < 0.001 versus ALB + SNL40; $ p < 0.001 versus ALB + SNL60; $β p < 0.001 versus MEM20, PGB30 and CLB20 (Two way ANOVA followed by Bonferroni's test)

damage to hippocampal memory formation. Groups with only auto-logous blood, compared with normal rats, showed a significant reduction in exploration times. Chronic SNL 60 mg/kg perse treatment showed no memory alteration as compared to normal rats. Posttreatment with SNL 40 mg/kg and SNL 60 mg/kg significantly improved the time of exploration. Treatment with SNL 60 mg / kg in combination with MEM 20 mg / kg increased the exploration time significantly and dose-dependently compared to SNL 60 mg / kg in combination with DNP 3 mg / kg, CLB 20 mg / kg and PGB 30 mg / kg (p < 0.001) (Fig. 8).

3.3. Neuroprotective effect of SNL on mitochondrial enzyme complexes (Complex I, II and V) and CoQ_{10} in ALB induced brain hemorrhagic rats

ALB mediated ICH-IVH compared to normal and SNL 60 mg/kg perse rats in rats with damaged mitochondrial enzyme complex (I, II, and IV) activities and levels of CoQ10. Nonetheless, as opposed to the ALB group 35 days of treatment with SNL 40 mg/kg and SNL 60 mg/kg substantially restored mitochondrial enzyme complex activity (I, II, and V) and CoQ10 levels. In addition, the combination of SNL 60 mg / kg with PGB 30 mg / kg significantly restored enzyme-complex enzyme activity (I, II and IV) and CoQ10 levels compared to SNL 60 mg / kg given in combination with DNP 3 mg / kg, MEM 20 mg / kg, and CLB

20 mg / kg (p < 0.001) (Table 1).

3.4. Neuroprotective effect of SNL on neurotransmitter levelsin ALB induced brain hemorrhagic rats

In contrast to the sham control group (p < 0.001), the group treated with ALB alone showed a low level of GABA and dopamine and a high level of glutamate. Significantly and dose-dependently, post-treatment with SNL 40 mg/kg and SNL 60 mg/kg for 35 days prevented increases in GABA, dopamine and glutamate levels (p < 0.001). The combination of SNL 60 mg/kg with MEM 20 mg/kg significantly improved dopamine levels and reduced the elevated levels of glutamate compared to SNL 60 mg/kg in combination with DNP 3, PGB 30 and CLB 20 (p < 0.001). The combination of SNL 60 mg / kg with PGB 30 mg / kg also lowered GABA levels in comparison with SNL 60 mg / kg in combination with MEM 20, DNP 3 and CLB 20 (p < 0.001) (Table 2).

3.5. Neuroprotective effect of SNL on acetylcholine and acetylcholinesterase levelsin ALB induced ICH-IVH in rats

The group treated with ALB alone showed a significantly low level of Ach and a high level of AchE when compared to the sham control group (p < 0.001). Post-treatment with SNL 40 mg / kg and SNL 60 mg
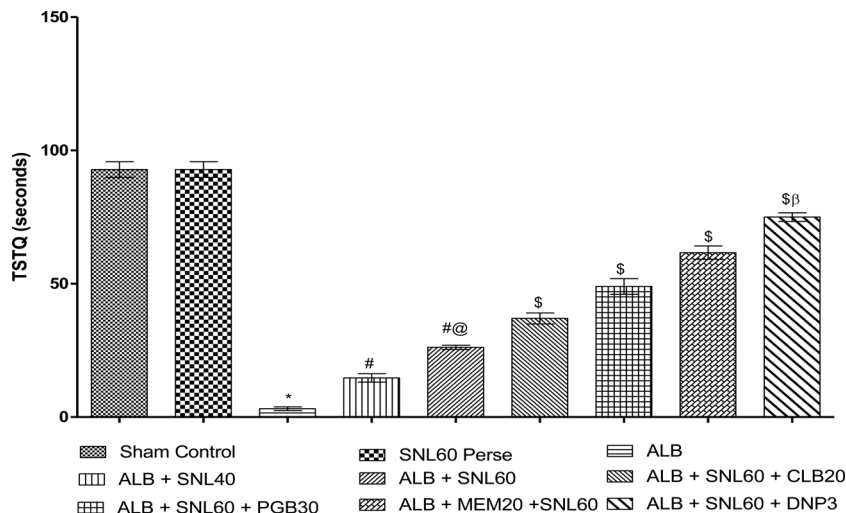

Fig. 4. Neuroprotective effect of SNL on time spent in target quadrant in ALB induced.
ICH-IVH in rats using morris water maze.
Data expressed as mean ± SEM (n = 6). * p < 0.001 versus sham control and SNL60 *perse*; # p < 0.001 versus ALB; #@ p < 0.001 versus ALB + SNL40; $ p < 0.001 versus ALB + SNL60; $β p < 0.001 versus MEM20, PGB30 and CLB20 (Two way ANOVA followed by Bonferroni's test)
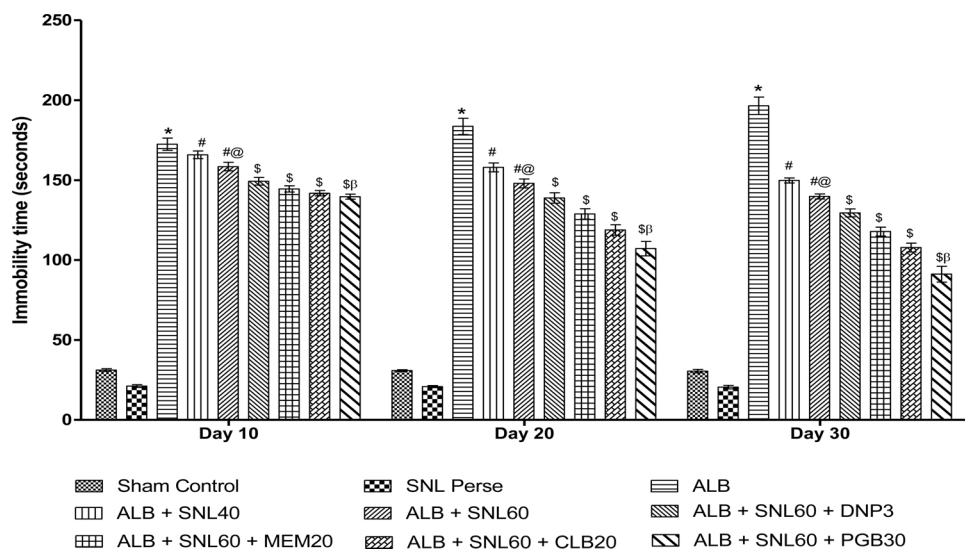
Fig. 5. Neuroprotective effect of SNL on immobility using forced swim test in ALB. induced ICH-IVH in rats.
Data expressed as mean ± SEM (n = 6). * p < 0.001 versus sham control and SNL60 *perse*; # p < 0.001 versus ALB; #@ p < 0.001 versus ALB + SNL40; $ p < 0.001 versus ALB + SNL60; $β p < 0.001 versus CLB20, MEM20, and DNP3 (Two way ANOVA followed by Bonferroni's test)

/ kg has substantially and dose-dependently prevented improvements in Ach and AchE (p < 0.001) levels for 35 days. In addition, the combination of SNL 60 mg / kg with DNP 3 mg / kg significantly improved Ach and decreased the elevated levels of AchE in contrast to SNL 60 given in combination with MEM 20 mg / kg, CLB 20 mg / kg and PGB 30 mg / kg (p < 0.001) (Table 3).

3.6. Neuroprotective effect of SNL on TNF-α, IL-6 and IL-1β levelsin ALB induced ICH IVH in rats

Intracerebroventricular administration of ALB significantly increased the level of pro-inflammatory markers i.e. TNF-α, IL-6 and IL-1β levels in the brain as compared to normal and SNL 60 mg/kg *perse* group. However, 35 days of treatment with SNL 40 mg/kg and SNL 60 mg/kg significantly and dose-dependently reduced the levels of TNF-α, IL-6, and IL-1β as compared to the ALB group. Further, combination of SNL 60 mg/kg with CLB 20 mg/kg significantly attenuated levels of TNF-α, IL-6 and IL-1β compared to SNL 60 given in combination with PGB 30 mg/kg, MEM 20 mg/kg and DNP 3 mg/kg (p < 0.001) (Table 4).

3.7. Neuroprotective effect of SNL on brain oxidative stress (SOD, nitrite, concentration, GSH, and MDA) in ALB induced ICH-IVH in rats

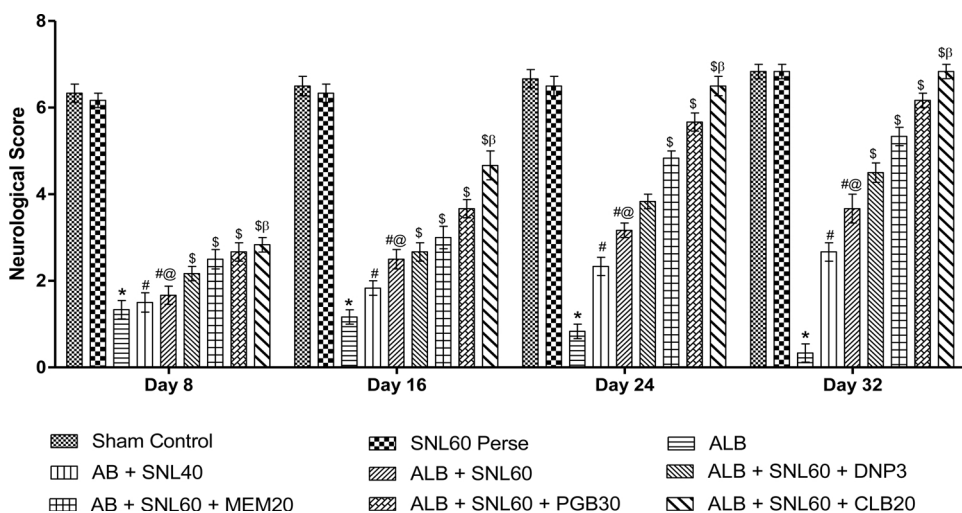The sham control group showed no significant impact on SOD

enzymes, the concentration of nitrite, GSH, and lipid peroxidation relative to SNL 60 mg/kg pers. However, the administration of ALB significantly increased levels of MDA, nitrite concentration, and depleted GSH and SOD enzymes as compared to the sham control group. 35 days of treatment with SNL 40 mg/kg and SNL 60 mg/kg significantly attenuated oxidative stress (decreased lipid peroxidation, nitrite concentration, and restored enzyme levels of GSH and SOD) compared to those in which only autologous blood was used. In comparison, the combination of SNL 60 mg / kg with PGB 30 mg / kg substantially reduced oxidative stress relative to SNL 60 in combination with DNP 3 mg / kg, MEM 20 mg / kg and CLB 20 mg / kg (p < 0.001) (Table 5).

3.8. Neuroprotective effect of SNL on gross pathological changes and hematoma size in ALB induced brain hemorrhagic rats

A Whole-brain observation

The autologous blood induced whole rat brain showed damaged clotted outer layer followed by breach meninges compared to sham and perse rats treated with SNL 60 mg/kg. In the sham control and SNL60 mg/kg *perse* grouped rats' brains showed optimally sized with clearly observable meninges. Furthermore, when compared with DNP 3 mg / kg, MEM 20 mg / kg and CLB 20 mg / kg treated rats, SNL 60 mg / kg in combination with PGB 30 mg / kg significantly improves morphological changes (Fig. 9).

Fig. 6. Neuroprotective effect of SNL on neurological score using beam crossing task in. ALB induced ICH-IVH in rats.
Data expressed as mean ± SEM (n = 6). * p < 0.001 versus sham control and SNL60 *perse*; # p < 0.001 versus ALB; #@ p < 0.001 versus ALB + SNL40; $ p < 0.001 versus ALB + SNL60; $β p < 0.001 versus CLB20, MEM20, and DNP3 (Two way ANOVA followed by Bonferroni's test)
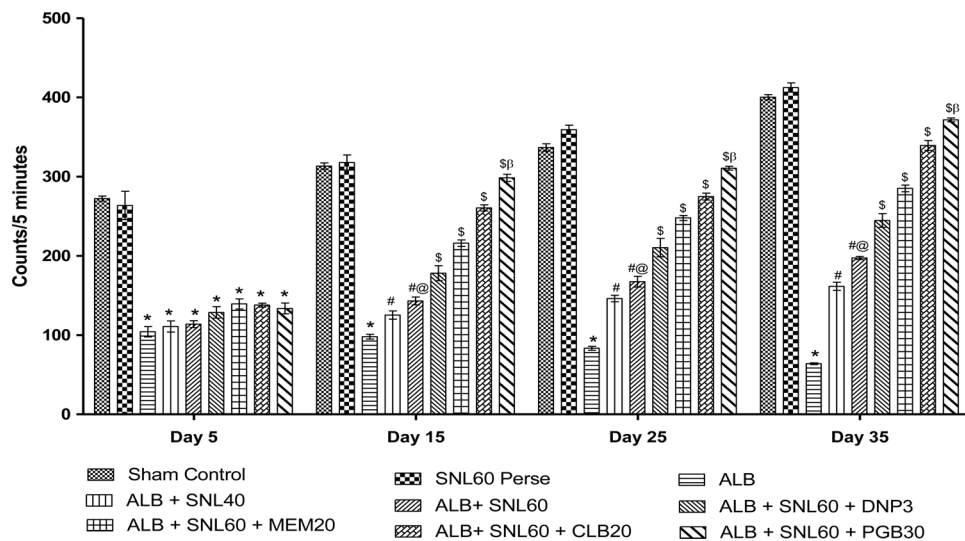
Fig. 7. Neuroprotective effect of SNL on locomotor activity using actophotometer in ALB. induced ICH-IVH in rats.
Data expressed as mean ± SEM (n = 6). * p < 0.001 versus sham control and SNL60 *perse*; # p < 0.001 versus ALB; #@ p < 0.001 versus ALB + SNL40; $ p < 0.001 versus ALB + SNL60; $β p < 0.001 versus CLB20, MEM20 and DNP3 (Two way ANOVA followed by Bonferroni's test)
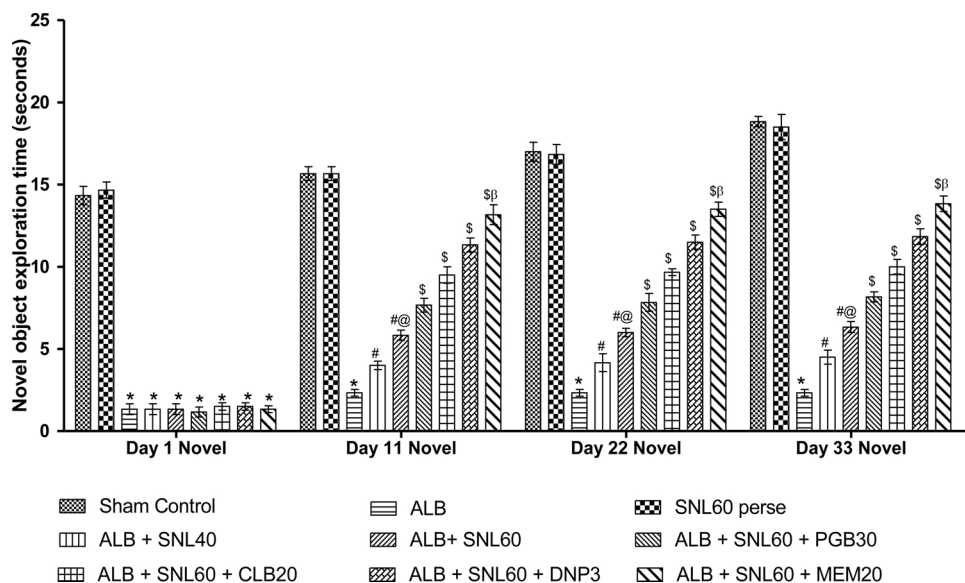

Fig. 8. Neuroprotective effect of SNL on exploration time using novel object recognition task in ALB induced ICH-IVH in rats.
Data expressed as mean ± SEM (n = 6). * p < 0.001 versus sham control and SNL60 *perse*; # p < 0.001 versus ALB; #@ p < 0.001 versus ALB + SNL40; $ p < 0.001 versus ALB + SNL60; $β p < 0.001 versus DNP3 CLB20, and PGB30 (Two way ANOVA followed by Bonferroni's test)

Table 1
Neuroprotective effect of SNL on mitochondrial enzyme complexes (Complex I, II and V) and CoQ$_{10}$ in ALB induced ICH-IVH in rats.

Groups	Complex- I (nM/mg protein)	Complex-II (nM/mg protein)	Complex-V (nM/mg protein)	CoQ$_{10}$ (nM/g protein)
Sham Control	14.0 ± 0.25	9.03 ± 0.24	735.0 ± 7.755	7.28 ± 0.06
SNL60 *perse*	14.1 ± 0.30	9.06 ± 0.19	735.0 ± 6.703	7.38 ± 0.15
ALB	2.83 ± 0.30*	1.20 ± 0.20*	226.8 ± 4.564*	0.83 ± 0.09*
ALB + SNL40	4.50 ± 0.42#	2.23 ± 0.19#	329.0 ± 16.48#	1.91 ± 0.23#
ALB + SNL60	6.00 ± 0.25#@	3.23 ± 0.17#@	376.7 ± 6.652#@	2.63 ± 0.15#@
ALB + SNL60 + CLB20	7.50 ± 0.42$	4.48 ± 0.09$	449.5 ± 9.986$	3.70 ± 0.21$
ALB + SNL60 + MEM20	8.95 ± 0.09$	5.38 ± 0.17$	528.7 ± 5.993$	4.68 ± 0.08$
ALB + SNL60 + DNP3	10.6 ± 0.33$	6.36 ± 0.15$	576.2 ± 7.981$	5.55 ± 0.13$
ALB + SNL60 + PGB30	12.3 ± 0.21$β	7.80 ± 0.22$β	636.2 ± 17.36$β	6.33 ± 0.08$β

Data expressed as mean ± SEM (n = 6). * p < 0.05 versus sham control and SNL60 *perse*; # p < 0.05 versus ALB; #@ p < 0.05 versus ALB + SNL40; $ p < 0.05 versus ALB + SNL60; $β p < 0.05 versus DNP3, MEM20, and CLB20 (One way ANOVA followed by Tukey's post hoc test).

B Brain section observation

During coronal sectioning, clearly observable brain tissue was observed in sham and SNL 60 mg/kg, perse treated rats. The coronal sections of ALB treated brains displayed cortical contusions, swellings, and severe subarachnoid hemorrhages associated with marked brain size reduction when compared to sham and perse-treated rats with SNL. In addition, compared to DNP 3 mg/kg, MEM 20 mg/kg and CLB 20

mg/kg treated rats, the combination of SNL 60 mg/kg with PGB 30 mg/kg substantially reduces autologous blood-mediated gross pathological changes (Fig. 10).

C Hematoma size

The sham control group showed no significant effect on the size of the hematoma compared with SNL 60 mg/kg, perse. However, the

Table 2
Neuroprotective effect of SNL on neurotransmitter levels in ALB induced ICH-IVH in rats.

Groups	Dopamine[a] (ng/mg tissue)	Glutamate[a] (ng/mg tissue)	Groups	GABA[b] (ng/mg tissue)
Sham Control	119.5 ± 8.097	84.67 ± 2.16	**Sham Control**	118.7 ± 7.508
SNL60 *Perse*	117.3 ± 6.159	85 ± 0.89	**SNL60 *Perse***	116.7 ± 7.508
AB	11.97 ± 1.347*	153.7 ± 3.77	**AB**	4.633 ± 1.793*
AB + SNL40	27.95 ± 7.844#	129.2 ± 1.16	**AB + SNL40**	16.3 ± 4.260#
AB + SNL60	44.7 ± 9.996#@	124 ± 2.098	**AB + SNL60**	29.13 ± 4.507#@
AB + SNL60 + CLB20	60.13 ± 10.40$	119.2 ± 2.04	**AB + SNL60 + CLB20**	39.13 ± 4.507$
AB + SNL60 + PGB30	75.92 ± 7.895$	111.8 ± 3.97	**AB + SNL60 + DNP3**	51.63 ± 4.096$
AB + SNL60 + DNP3	91.67 ± 5.837$	104.3 ± 1.862	**AB + SNL60 + MEM20**	64.13 ± 6.400$
AB + SNL60 + MEM20	107.7 ± 10.44$β	92 ± 0.8944	**AB + SNL60 + PGB30**	75.8 ± 6.047$β

[a] Data expressed as mean ± SEM (n = 6). * $p < 0.05$ versus sham control and SNL60 *perse*; # $p < 0.05$ versus ALB; #@ $p < 0.05$ versus ALB + SNL40; $ $p < 0.05$ versus ALB + SNL60; $β $p < 0.05$ versus DNP3, PGB30 and CLB20 (One way ANOVA followed by Tukey's post hoc test).

[b] Data expressed as mean ± SEM (n = 6). * $p < 0.05$ versus sham control and SNL60 *perse*; # $p < 0.05$ versus ALB; #@ $p < 0.05$ versus ALB + SNL40; $ $p < 0.05$ versus ALB + SNL60; $β $p < 0.05$ versus MEM20, DNP3 and CLB20 (One way ANOVA followed by Tukey's post hoc test).

Table 3
Neuroprotective effect of SNL on acetylcholine and acetylcholinesterase levels in ALB induced ICH-IVH in rats.

Groups	AchE (μmol/mg protein)	Ach (μmol/mg protein)
Sham Control	4.33 ± 3.67	8.71 ± 0.56
SNL60 *Perse*	4.33 ± 3.67	8.63 ± 0.95
ALB	94.5 ± 6.41*	0.21 ± 0.11*
ALB + SNL40	79.67 ± 8.86#	1.45 ± 0.45#
ALB + SNL60	65.0 ± 8.87#@	2.71 ± 0.18#@
ALB + SNL60 + PGB30	51.17 ± 6.49$	3.96 ± 0.56$
ALB + SNL60 + CLB20	37.2 ± 10.08$	5.38 ± 0.79$
ALB + SNL60 + MEM20	23.1 ± 5.29$	6.63 ± 0.72$
ALB + SNL60 + DNP3	9.23 ± 2.280$β	8 ± 0.70$β

Data expressed as mean ± SEM (n = 6). * $p < 0.05$ versus sham control and SNL60 *perse*; # $p < 0.05$ versus ALB; #@ $p < 0.05$ versus ALB + SNL40; $ $p < 0.05$ versus ALB + SNL60; $β $p < 0.05$ versus MEM20, CLB20 and PGB30 (One way ANOVA followed by Tukey's post hoc test).

Table 4
Effect of SNL on TNF-α, IL-6 and IL-1β levels in ALB induced ICH-IVH in rats.

Groups	Neuroinflammatory Markers		
	TNFα pg/mg protein	IL-1β pg/mg protein	IL-10 pg/mg protein
Sham Control	100.0 ± 2.88	73.17 ± 2.52	58.83 ± 0.54
SNL60 *perse*	99.83 ± 2.83	75.67 ± 2.21	58.50 ± 0.56
ALB	300.8 ± 3.27*	577.5 ± 6.72*	24.17 ± 1.16*
ALB + SNL40	263.3 ± 5.11#	478.3 ± 7.50#	33.17 ± 0.83#
ALB + SNL60	244.3 ± 3.11#@	430.8 ± 7.89#@	38.50 ± 0.56#@
ALB + SNL60 + DNP3	226.3 ± 3.26$	363.7 ± 4.21$	42.50 ± 0.42$
ALB + SNL60 + MEM20	204.0 ± 3.05$	315 ± 2.955$	48.33 ± 0.49$
ALB + SNL60 + PGB30	180.8 ± 3.00$	244.7 ± 7.90$	52.00 ± 0.57$
ALB + SNL60 + CLB20	160.0 ± 3.92$β	190.2 ± 5.57$β	55.17 ± 0.47$β

Data expressed as mean ± SEM (n = 6). * $p < 0.05$ versus sham control and SNL60 *perse*; # $p < 0.05$ versus ALB; #@ $p < 0.05$ versus ALB + SNL40; $ $p < 0.05$ versus ALB + SNL60; $β $p < 0.05$ versus PGB30, MEM20, and DNP3 (One way ANOVA followed by Tukey's post hoc test).

administration of intracerebroventricular ALB significantly increased the size of hematoma compared to the sham control group and SNL 60 mg/kg perse. Treatment with SNL 40 mg/kg and SNL 60 mg/kg significantly reduced the size of the hematoma compared to those groups where only autologous blood was used. In addition, the combination of SNL 60 mg/kg with PGB 30 mg/kg substantially reduced hematoma size compared to SNL 60 in combination with DNP 3 mg/kg, MEM 20 mg/kg and CLB 20 mg/kg (p < 0.001) (Fig. 11).

4. Discussion

The present study shows SNL's neuroprotective potential against ALB-induced combined ICH-IVH model in rats. Besides, chronic treatment with SNL 60 mg/kg alone and in combination with standard drug therapy such as MEM 20 mg/kg, DNP 3 mg/kg, PGB 30 mg/kg, and CLB 20 mg/kg demonstrated the neuroprotective effect in improving various ICH-IVH-related pathological hallmarks. In recent decades, the outcome of ICH, the most severe form of stroke, has not improved (Van Asch et al., 2010), and treatment options are still mainly limited to supportive therapy. Surgical treatment options were mostly unsuccessful, particularly in cases where hemorrhage breaks into the ventricular system. A combined ICH-IVH model is a novel approach that effectively and reliably mimics intraventricular-associated parenchymal bleeding induced through a single autologous blood injection. This combined ICH-IVH model was validated and characterized using biochemical analysis. The model also produced emotional, behavioral, and cognitive deficits, closely mimicking the effects of human hemorrhage in those brain regions.

In our findings, twenty microliters of ALB were injected into rat brain for the induction of ICH-IVH. Our protocol duration was 35 days, however, and autologous blood volume was very low, with 20 microliters of ALB causing sufficient blood clotting leading to low mortality rates (5.4 %), hematoma formation and ventricular enlargement compared to other studies where high mortality was observed with increasing blood volume. In the pathophysiology of a brain hemorrhage, mitochondrial dysfunction, oxidative stress, and neuroinflammation have been well reported (Ostrowski et al., 2007). Hematoma development resulted in cognitive impairment, increased oxidative stress (as shown by elevated lipid peroxidation-MDA, nitric concentration and decreased glutathione depletion, SOD), impaired mitochondrial enzyme-complex activities (I, II and V) with reduced levels of CoQ10 and increased neuroinflammation (TNF-α, IL-1β, IL-10) in the hemorrhagic brain.

Despite having neuroprotective, anti-inflammatory, and anti-oxidant effects, SNL's exact action mechanism has not yet been properly understood (Yan et al., 2015). In the current study, 35-day SNL treatment significantly improves behavioral and motor impairment, oxidative damage, neuroinflammation and restored mitochondrial enzyme complex activity (I, II and V) in hemorrhagic rats, indicating its multiple target activities at various cellular and molecular cascades of complex ICH-IVH pathogenesis responsible for its neuroprotective effectiveness

CLB 20 demonstrated well in ischemia models for its anti-inflammatory, anti-apoptotic, and neuroprotective effects (Chu and Jeong, 2004). Cerebral hemorrhage associated with caspase activation and the release of prostaglandin responsible for cell death and inflammation of the neurons (Sinn and Lee, 2007). Therefore, prolonged

Table 5
Neuroprotective effect of SNL on brain oxidative stress (SOD, nitrite concentration, GSH and lipid peroxidation (MDA)) in ALB induced ICH-IVH in rats.

Groups	SOD (U/mg)	Nitrite (µg/mL)	GSH (µmol/mg protein)	MDA (nM/mg protein)
Sham Control	45 ± 1.414	301.5 ± 29.49	0.95 ± 0.024	0.5833 ± 0.487
SNL60 *perse*	43.67 ± 0.8165	309.7 ± 20.34	0.96 ± 0.027	0.7167 ± 0.479
ALB	12.67 ± 2.160*	818.3 ± 35.60*	0.01 ± 0.005*	13.03 ± 1.193*
ALB + SNL40	17.67 ± 2.582[#]	740.8 ± 21.28[#]	0.16 ± 0.033[#]	11.23 ± 1.120[#]
ALB + SNL60	22.67 ± 2.658[#@]	671.2 ± 58.72[#@]	0.31 ± 0.059[#@]	9.35 ± 0.7176[#@]
ALB + SNL60 + CLB20	27.67 ± 3.141[$]	584.2 ± 21.56[$]	0.45 ± 0.126[$]	7.583 ± 0.9453[$]
ALB + SNL60 + MEM20	32.83 ± 2.787[$]	517.3 ± 21.58[$]	0.61 ± 0.069[$]	5.833 ± 1.181[$]
ALB + SNL60 + DNP3	37.83 ± 1.472[$]	442 ± 20.91[$]	0.75 ± 0.099[$]	4.033 ± 1.041[$]
ALB + SNL60 + PGB30	42.67 ± 4.227[$β]	373.2 ± 16.46[$β]	0.91 ± 0.040[$β]	2.033 ± 0.4590[$β]

Data expressed as mean ± SEM (n = 6). * $p < 0.05$ versus sham control and SNL60 *perse*; # $p < 0.05$ versus ALB; #@ $p < 0.05$ versus ALB + SNL40; $ $p < 0.05$ versus ALB + SNL60; $β $p < 0.05$ versus DNP3, MEM20 and CLB20 (One way ANOVA followed by Tukey's post hoc test).

treatment with CLB 20 in conjunction with SNL 60 decreased the elevated neuroinflammatory markers such as TNF-α, IL-1β, IL-10 for 35 days and also increased the neurological score in the beam crossing test relative to other therapies and disease classes, indicating its possible neuroprotective effects in the prevention of inflammation and neuronal mortality in patients.

The early period of ICH-IVH includes the accumulation of glutamate in the perihematomal region's extracellular space, which results in NMDA overstimulation causing excessive calcium inflow and subsequent excitotoxic injury (Qureshi and Ali, 2003). MEM 20, a noncompetitive NMDA receptor antagonist, reported reducing excitotoxicity-induced injury and inhibiting hematoma expansion in combination with a decrease of the metalloproteinase-9 matrix (MMP-9) (Lee and Chu, 2006). In this study MEM 20 significantly improved
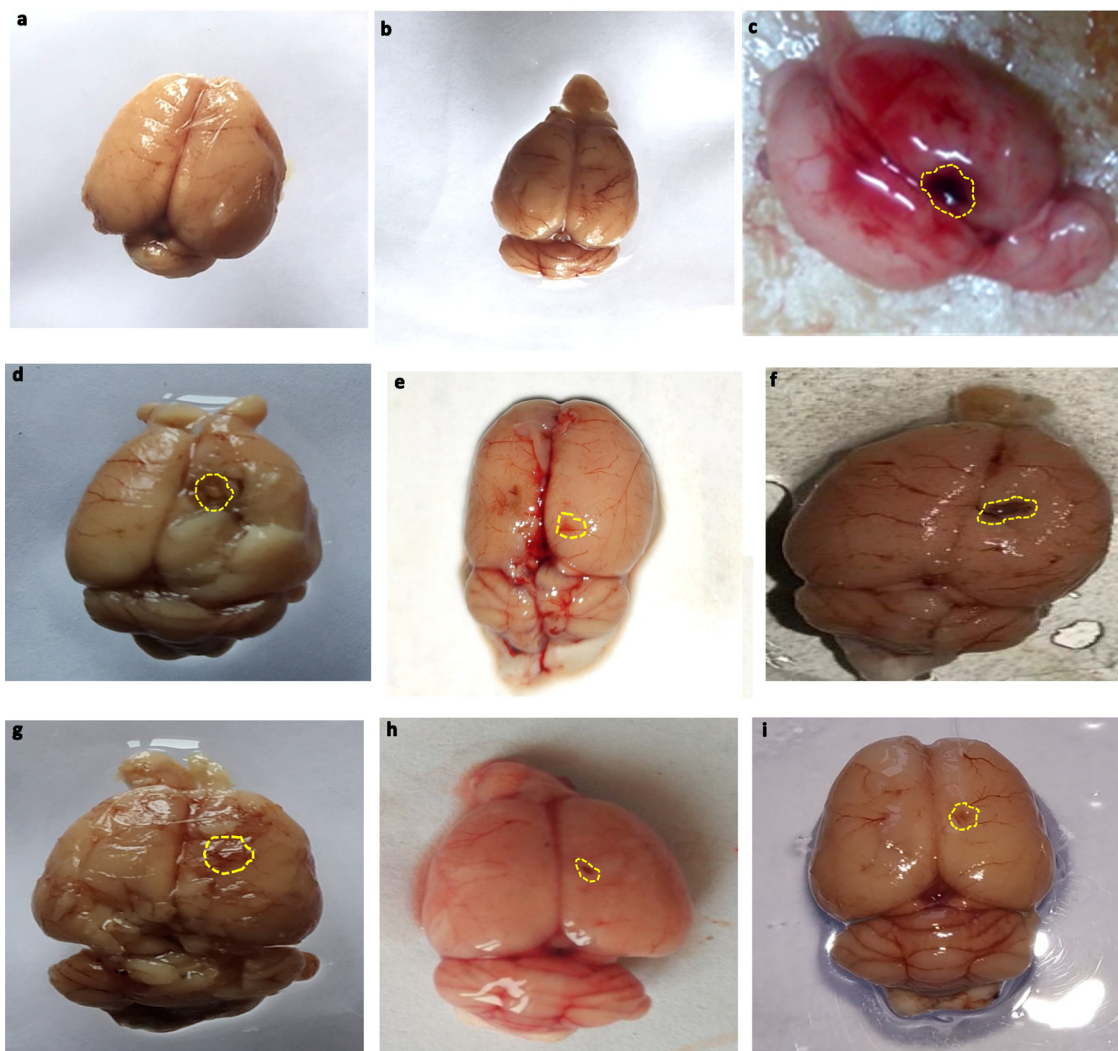

Fig. 9. Neuroprotective effect of SNL on gross pathological changes (whole rat brain) in ALB induced brain hemorrhagic rats.
(a) Sham control i. Cerebral cortex ii. Hippocampus iii. Basal ganglia (b) SNL *perse* (c) ALB (d) ALB + SNL 40 (e) ALB + SNL 60 (f) ALB + SNL 60 + CLB 2 (g) ALB + SNL 60 + MEM 20 (h) ALB + SNL 60 + DNP 3 (i) ALB + SNL 60 + PGB 30 (Scale bar = 2 mm)
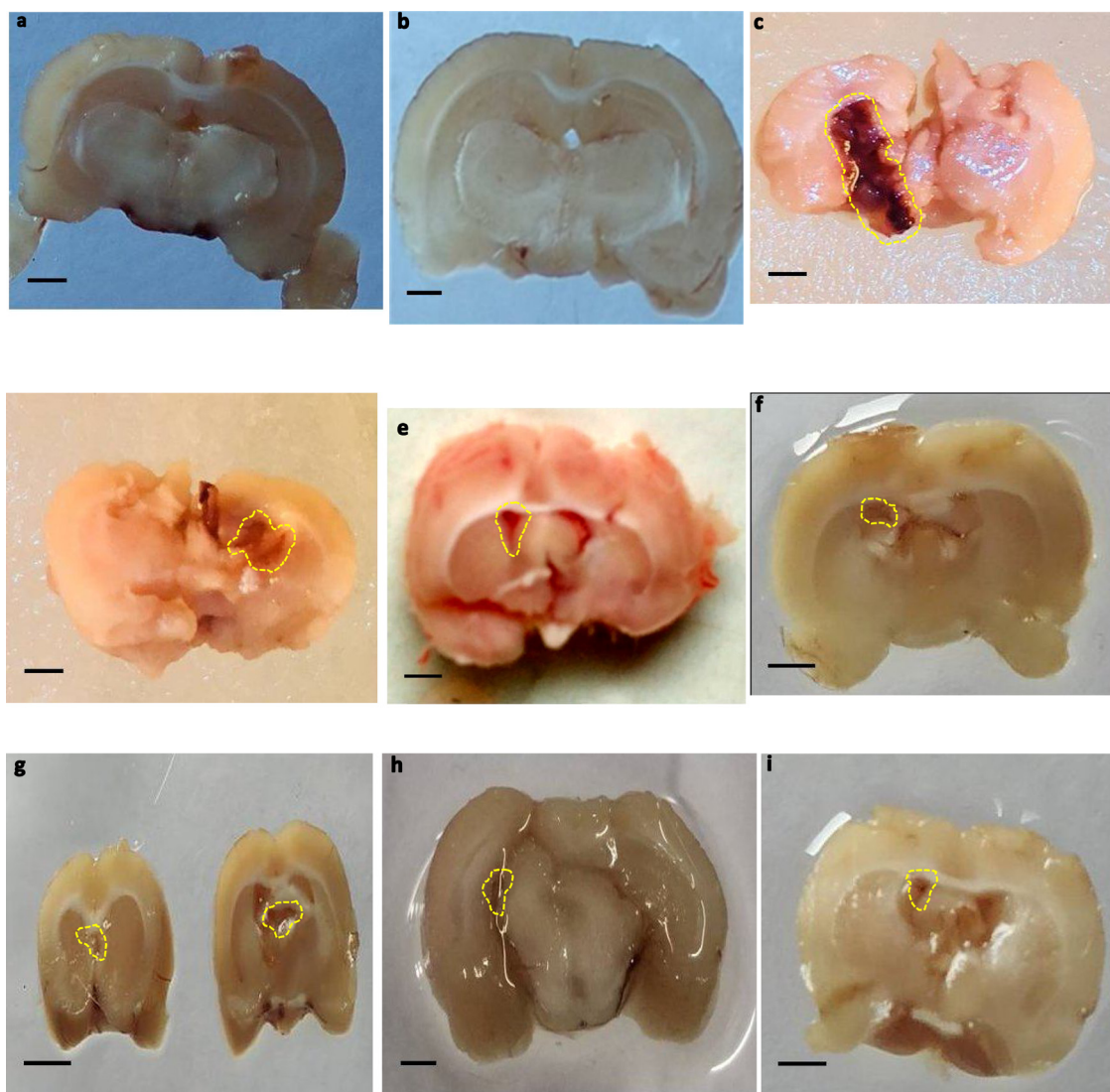Note: Yellow circles are pointing to the site of the brain injury

Fig. 10. Neuroprotective effect of SNL on gross pathological changes (brain section) in ALB induced brain hemorrhagic rats.
(a) Sham control (b) SNL *perse* (c) ALB (d) ALB + SNL 40 (e) ALB + SNL 60 (f) ALB + SNL 60 + CLB 2 (g) ALB + SNL 60 + MEM 20 (h) ALB + SNL 60 + DNP 3 (i) ALB + SNL 60 + PGB 30 (Scale bar = 5 mm).
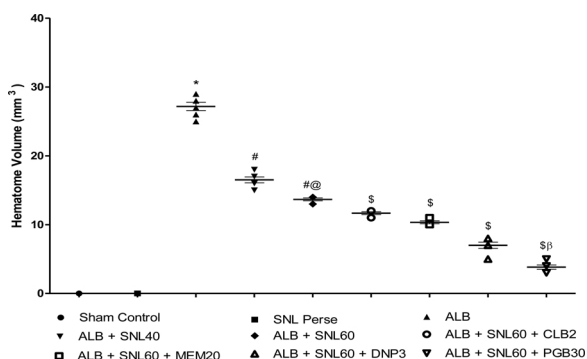Note: Yellow circles are pointing to the hematoma size

Fig. 11. Neuroprotective effect of SNL on hematoma size in ALB induced brain hemorrhagic rats.
Data expressed as mean ± SEM (n = 6). * $p < 0.05$ versus sham control and SNL60 *perse*; # $p < 0.05$ versus ALB; #@ $p < 0.05$ versus ALB + SNL40; \$ $p < 0.05$ versus ALB + SNL60; \$β $p < 0.05$ versus DNP3, MEM20 and CLB2 (One way ANOVA followed by Bonferroni's test)

recognition in NOR when used in combination with SNL 60 showing functional recovery with a decrease in glutamate levels and an increase in dopamine levels, providing new insight into the treatment of ICH-IVH with NMDAR blockers.

Donepezil, a specifically central acetylcholinesterase inhibitor, reported potentiating learning in stroke subjects by amplifying cholinergic feedback from Meynert's nucleus basalis into the cerebral cortex (Nadeau et al., 2004). Hematoma formation can cause contusion of these structures, resulting in reduced Ach synthesis and transportation to different parts of the brain, thereby affecting learning and memory (Zhang and Plotkin, 2004; Myhrer, 2003). The present investigation reveals that when given in combination with SNL 60, DNP 3 increases the escape latency and reduces the time spent in a spatial navigation task in MWM in the target quadrant. It also reduced the elevated levels of AChE and raised the levels of Ach leading to cognitive changes by increasing the cholinergic system in the basal forebrain.

The neuroprotective effect of PGB 30 with epilepsy, anxiety and neuropathic pain is well reported (Park et al., 2009). Besides being a structural analog of GABA, it has no direct action on GABA pathways. It is a novel ligand of alpha-2-delta (α2-δ) subunits of voltage-gated calcium channels (VGCC) using an animal model to exercise

anticonvulsant, analgesic, and anxiolytic action. In the current study PGB 30 improved body weight, locomotion, and mobility time in FST in combination with SNL. It also preserved the complex functions of the mitochondrial, decreased oxidative stress, increased GABA levels relative to other standard drugs in conjunction with SNL. Confirming PGB 30 beneficial effects present in specific pathological ICH-IVH pathways. These results suggest that ALB mediated ICH-IVH causes complex mitochondrial dysfunction and increased oxidative stress, inflammatory cytokines, and altered neurotransmitter levels in rat brain, where chronic SNL administration, as a precursor to CoQ10, strengthened these neuropathological defects. In addition, chronic treatment with SNL alone and in conjunction with standard drugs (DNP 3, MM 20, CLB 20, PGB 30) significantly reduces oxidative stress, inflammatory cytokines and restores the amount of neurotransmitters in the brain of rats and restores mitochondrial functioning by improving the production of CoQ10 and ATP providing a better functional recovery. In our research, morphological and gross pathological changes followed by neurological functions and expressions of different biomarkers were examined after induction of hemorrhage in the rat brain which shows the neuroprotective effect of SNL, indicating the satisfactory repeatability and controllability of this novel animal model.

There are limitations to the current study. We perform a critical technique of a combined ICH-IVH model and there is no experimental animal model near the exact clinical conditions that can be 100 percent. Furthermore, the incapability of high-resolution MRI in this study made it difficult to distinguish between ICH and IVH.

5. Conclusion

In conclusion, ICH-IVH animals developed severe learning and memory loss, motor impairment followed by complex mitochondrial enzyme dysfunction, neurochemical disruptions, oxidative stress elevation, and increased neuroinflammatory markers. Chronic SNL therapy provides a neuroprotective effect by improving behavioral and neurochemical deficits. In addition, SNL shows a synergistic effect when used in post brain hemorrhagic conditions in rats in conjunction with standard drug therapy (DNP 3, MM 20, CLB 20, PGB 30). Therefore, SNL could be a possible therapeutic strategy associated with post-brain hemorrhagic behavioral and neurochemical changes to improve neuronal dysfunction.

6. Author contributions

Ms. Kajal Rajdev: M.Pharm Research Scholar, Neuropharmacology Division
Contribution: Thesis work, Performed experimental animal studies, compilation of research statistical data
Mr. Ehraz Mehmood Siddiqui: M.Pharm Research Scholar, Neuropharmacology Division
Contribution: Prepare revised manuscript and compilation of research statistical data
Mr. Kuldeep Singh Jadaun: M.Pharm Research Scholar, Neuropharmacology Division
Contribution: Prepare revised manuscript and removal of grammatical errors
Dr. Sidharth Mehan: PhD, M.Pharm, Neuropharmacology Division
Contribution: Original research hypothesis, guide and compilation of all manuscript data

Conflict of Interest

The authors have no conflict of interest to report.

References

Arab, M., Bahramian, B., Schindeler, A., Fathi, A., Valtchev, P., McConchie, R., Dehghani, F., 2019. A benign process for the recovery of solanesol from tomato leaf waste. Heliyon 5 (4), e01523.

Aronowski, J., Hall, C.E., 2005. New horizons for primary intracerebral hemorrhage treatment: experience from preclinical studies. Neurol. Res. 27 (3), 268–279.

Aronowski, J., Zhao, X., 2011. Molecular pathophysiology of cerebral hemorrhage: secondary brain injury. Stroke 42 (6), 1781–1786.

Barcelos, I.P.D., Haas, R.H., 2019. CoQ10 and aging. Biology 8 (2), 28.

Berman, S.B., Hastings, T.G., 1999. Dopamine oxidation alters mitochondrial respiration and induces permeability transition in brain mitochondria: implications for Parkinson's disease. J. Neurochem. 73 (3), 1127–1137.

Bhardwaj, M., Kumar, A., 2016. Neuroprotective mechanism of coenzyme Q_{10} (CoQ$_{10}$) against PTZ induced kindling and associated cognitive dysfunction: possible role of microglia inhibition. Pharmacol. Rep. 68 (6), 1301–1311.

Brunswick, A.S., Hwang, B.Y., Appelboom, G., Hwang, R.Y., Piazza, M.A., Connolly, E.S.Jr., 2012. Serum biomarkers of spontaneous intracerebral hemorrhage induced secondary brain injury. J. Neurol. Sci. 321, 1–10.

Caceres, J.A., Goldstein, J.N., 2012. Intracranial hemorrhage. Emerg. Med. Clin. North Am. 30 (3), 771.

Cai, J., et al., 2015. Progesterone alleviates acute brain injury via reducing apoptosis and oxidative stress in a rat experimental subarachnoid hemorrhage model. Neurosci. Lett. 600, 238–243.

Campbell, R., Freitag, S., Bryan, G.J., Stewart, D., Taylor, M.A., 2016. Environmental and genetic factors associated with solanesol accumulation in potato leaves. Front. Plant Sci. 7, 1263.

Chaudhary, N., Gemmete, J.J., Thompson, B.G., Xi, G., Pandey, A.S., 2013. Iron–potential therapeutic target in hemorrhagic stroke. World Neurosurg. 79 (1), 7.

Chu, K., Jeong, S.W., et al., 2004. Celecoxib induces functional recovery after intracerebral hemorrhage with reduction of brain edema and perihematomal cell death. J. of Cerebral Blood Flow Metabol. 24 (8), 926–933.

DeLegge, M.H., Smoke, A., 2008. Neurodegeneration and inflammation. Nut. Clin. Prac. 23 (1), 35–41.

Donzanti, B.A., Yamamoto, B.K., 1988. An improved and rapid HPLC-EC method for the isocratic separation of amino acid neurotransmitters from brain tissue and microdialysis perfusates. Life Sci. 43 (11), 913–922.

Duan, X., Wen, Z., Shen, H., Shen, M., Chen, G., 2016. Intracerebral hemorrhage, oxidative stress, and antioxidant therapy. Oxid. Med. Cell. Longev.

Ellman, G.L., 1959. Tissue sulfhydryl groups. Arch Biochem Biophys 82, 70–77.

Ellman, G.L., Courtney, K.D., Andres Jr., V., Featherstone, R.M., 1961. A new and rapid colorimetric determination of acetylcholinesterase activity. Biochemical Pharmacol. 7 (2), 88–95.

Findlay, J.Max., 2011. Intraventricular hemorrhage. Therapy 70, 1349–1357.

Fiorella, D., Zuckerman, S.L., Khan, I.S., Kumar, N.G., Mocco, J., 2015. Intracerebral hemorrhage: a common and devastating disease in need of better treatment. World Neurosurgery 84 (4), 1136–1141.

Gao, F., Liu, F., Chen, Z., Hua, Y., Keep, R.F., Xi, G., 2014. Hydrocephalus after intraventricular hemorrhage: the role of thrombin. J. Cerebral Blood Flow Metabol. 34 (3), 489–494.

Gong, C., Boulis, N., Qian, J., Turner, D.E., Hoff, J.T., Keep, R.F., 2001. Intracerebral hemorrhage-induced neuronal death. Neurosurgery 48 (4), 875–883.

Gornall, A.G., Bardawill, C.J., David, M.M., 1949. Determination of serum proteins by means of the biuret reaction. J. Boil. Chem. 177 (2), 751–766.

Green, L.C., Wagner, D.A., Glogowski, J., Skipper, P.L., Wishnok, J.S., Tannenbaum, S.R., 1982. Analysis of nitrate, nitrite, and [15N] nitrate in biological fluids. Anal Biochem. 126, 131–138.

Guo, Y., Ni, J.R., Huang, W., 2008. Comparison on bioactivities of solanesol extracted from tobacco leaves by different methods. J. Anhui Agric. Sci. 36, 6356–6359.

Hu, X., Tao, C., Gan, Q., Zheng, J., Li, H., You, C., 2016. Oxidative stress in intracerebral hemorrhage: sources, mechanisms, and therapeutic targets. Oxid. Med. Cellular Longevity 2016.

Hussein, J.I.H.A.N., et al., 2012. Brain neurotransmitters in diabetic rats treated with CO enzyme Q_{10}. Int. J. Pharm. Pharm. Sci. 4, 554–556.

Jamwal, S., Kumar, P., 2016. Spermidine ameliorates 3-nitropropionic acid (3-NP)-induced striatal toxicity: possible role of oxidative stress, neuroinflammation, and neurotransmitters. Physiology & behavior 155, 180–187.

Kafi, H., Salamzadeh, J., Beladimoghadam, N., Sistanizad, M., Kouchek, M., 2014. Study of the neuroprotective effects of memantine in patients with mild to moderate ischemic stroke. Iranian J. Pharm. Res.: IJPR 13 (2), 591.

Kanamoto, T., et al., 2019. Effect of ocular hypertension on D-β-Aspartic acid-containing proteins in the retinas of rats. J. Ophthalmol. 2019.

Kim, S., Han, S.C., Gallan, A.J., Hayes, J.P., 2017. Neurometabolic indicators of mitochondrial dysfunction in repetitive mild traumatic brain injury. Concussion 2 (3), CNC45.

Kim-Han, J.S., Kopp, S.J., Dugan, L.L., Diringer, M.N., 2006. Perihematomal mitochondrial dysfunction after intracerebral hemorrhage. Stroke 37, 2457–2462.

King, T.E., 1967b. Preparations of succinate—cytochrome c reductase and the cytochrome *b*-c1 particle, and reconstitution of succinate-cytochrome c reductase. Methods in Enzymology Vol. 10. Academic Press, pp. 216–225.

King, T.E., Howard, R.L., 1967a. Preparations and properties of soluble NADH dehydrogenases from cardiac muscle. Methods in Enzymology Vol. 10. Academic Press, pp. 275–294.

Kono, Y., 1978. Generation of superoxide radical during autoxidation of hydroxylamine and an assay for superoxide dismutase. Archives Bbiochem. Biophys. 186 (1), 189–195.

Kotipalli, K.P., Rao, N.C.V., Raj, K., 2008. Estimation of solanesol in tobacco and non-tobacco plants from Solanaceae family. J. Med. Aroma Plant Sci. 30, 65–68.

Lee, S.T., Chu, K., et al., 2006. Memantine reduces hematoma expansion in experimental intracerebral hemorrhage, resulting in functional improvement. J. Cerebral Blood Flow Metabol. 26 (4), 536–544.

Liu, M., Zhang, C., Liu, W., Luo, P., Zhang, L., Wang, Y., Wang, Z., Fei, Z., 2015. A novel rat model of blast-induced traumatic brain injury simulating different damage degree: implications for morphological, neurological, and biomarker changes. Front. Cellular Neurosci. 9, 168.

Lu, Q., Huang, L., ZhuGe, Q., 2015. A rat model of intracerebral hemorrhage induced by collagenase IV. Bio-protocol 5, e1541.

Marinkovic, I., Tatlisumak, T., 2014. A novel combined model of intracerebral and intraventricular hemorrhage using autologous blood-injection in rats. Neuroscience 272, 286–294.

Masanic, C.A., Bayley, M.T., Simard, M., 2001. Open-label study of donepezil in traumatic brain injury. Arch. Phys. Med. Rehabilit. 82 (7), 896–901.

Matthews, R.T., Yang, L., Browne, S., Baik, M., Beal, M.F., 1998. Coenzyme Q$_{10}$ administration increases brain mitochondrial concentrations and exerts neuroprotective effects. Proc. Natl. Acad. Sci. U. S. A. 95, 8892–8897.

Mehan, S., Monga, V., Rani, M., Dudi, R., Ghimire, K., 2018. Neuroprotective effect of solanesol against 3-nitropropionic acid-induced Huntington's disease-like behavioral, biochemical, and cellular alterations: restoration of coenzyme-Q$_{10}$-mediated mitochondrial dysfunction. Indian J. Pharmacol. 50 (6), 309–319. https://doi.org/10.4103/ijp.IJP_11_18.

Myhrer, T., 2003. Neurotransmitter systems involved in learning and memory in the rat: a meta-analysis based on studies of four behavioral tasks. Brain Res. Rev. 41 (2–3), 268–287.

Nadeau, S.E., et al., 2004. Donepezil as an adjuvant to constraint-induced therapy for upper-limb dysfunction after stroke: an exploratory randomized clinical trial. J. Rehabilit. Res. Develop. 41 (4).

Nedergaard, M., Klinken, L., Paulson, O.B., 1983. Secondary brain stem hemorrhage in stroke. Stroke 14 (4), 501–505.

Okamoto, T., Fukui, K., Nakamoto, M., Kishi, T., Okishio, T., Yamagami, T., Kanamori, N., Kishi, H., Hiraoka, E., 1985. High-performance liquid chromatography of coenzyme Q-related compounds and its application to biological materials. J. Chromat. B: Biomed. Sci. Appl. 342, 35–46.

Orsucci, D., Mancuso, M., Ienco, E.C., LoGerfo, A., Siciliano, G., 2011. Targeting mitochondrial dysfunction and neurodegeneration by means of coenzyme Q$_{10}$ and its analogues. Current Med. Chem. 18 (26), 4053–4064.

Park, H.K., Lee, S.H., Chu, K., Roh, J.K., 2009. Effects of celecoxib on volumes of hematoma and edema in patients with primary intracerebral hemorrhage. J. Neurol. Sci. 279 (1–2), 43–46.

Prentice, H., Modi, J.P., Wu, J.-Y., 2015. Mechanisms of neuronal protection against excitotoxicity, endoplasmic reticulum stress, and mitochondrial dysfunction in stroke and neurodegenerative diseases. Oxid. Med. Cell. Long. 2015, 1–7.

Qin, B., Liu, L., Pan, Y., Zhu, Y., Wu, X., Song, S., Han, G., 2017. PEGylatedsolanesol for oral delivery of coenzyme Q$_{10}$. J. Agric. Food Chem. 65 (16), 3360–3367.

Qin, Y., Li, G.L., Xu, X.H., Sun, Z.Y., Gu, J.W., Gao, F.B., 2018. Brain structure alterations and cognitive impairment following repetitive mild head impact: an in vivo MRI and behavioral study in rat. Behav. Brain Res. 340, 41–48.

Qureshi, A.I., Ali, Z., et al., 2003. Extracellular glutamate and other amino acids in experimental intracerebral hemorrhage: an in vivo microdialysis study. Critical Care Med. 31 (5), 1482–1489.

Qureshi, A.I., Tuhrim, S., Broderick, J.P., Batjer, H.H., Hondo, H., Hanley, D.F., 2001. Spontaneous intracerebral hemorrhage. New England J. Med. 344 (19), 1450–1460.

Rahajeng, B., Ikawati, Z., Andayani, T.M., Dwiprahasto, I., 2018. The effect of Pregabalin on the quality of life in patients with central post-stroke pain. J. Young Pharm. 10 (2), 222.

Roh, J.H., Ko, I.G., Kim, S.E., Lee, J.M., Ji, E.S., Kim, J.H., Chang, H.K., Lee, S.K., Kim, K.H., 2016. Treadmill exercise ameliorates intracerebral hemorrhage-induced depression in rats. J. Exercise Rehabilit. 12 (4), 299.

Rynkowski, M.A., Kim, G.H., et al., 2008. A mouse model of intracerebral hemorrhage using autologous blood infusion. Nature Protocols 3 (1), 122.

Sa´ndor, P.S., Clemente, L.D., Coppola, G., Saenger, U., Fumal, A., Magis, D., Seidel, L., 2005. Efficacy of coenzyme Q$_{10}$ in migraine prophylaxis: a randomized controlled trial. Neurology 64, 713–715.

Sharma, R., Rahi, S., Mehan, S., 2019. Neuroprotective potential of solanesol in intracerebroventricular propionic acid induced experimental model of autism: insights from behavioral and biochemical evidence. Toxicol Rep 2019 (6), 1164–1175.

Sinar, E.J., Mendelow, A.D., Graham, D.I., Teasdale, G.M., 1987. Experimental intracerebral hemorrhage: effects of a temporary mass lesion. J. Neurosurg. 66 (4), 568–576.

Singh, N., Bansal, Y., Bhandari, R., Marwaha, L., Singh, R., Chopra, K., Kuhad, A., 2017. Naringin reverses neurobehavioral and biochemical alterations in intracerebroventricular collagenase-induced intracerebral hemorrhage in rats. Pharmacology 100 (3-4), 172–187.

Sinn, D.I., Lee, S.T., et al., 2007. Combined neuroprotective effects of celecoxib and memantine in experimental intracerebral hemorrhage. Neuroscience Lett. 411 (3), 238–242.

Song, Y., Jun, J.H., 2017. Effect of pregabalin administration upon reperfusion in a rat model of hyperglycemic stroke: mechanistic insights associated with high-mobility group box 1. PloS one 12 (2), e0171147.

Sook Kim-Han, J., Kopp, S.J., Dugan, L.L., Diringer, M.N., 2006. Perihematomal mitochondrial dysfunction after intracerebral hemorrhage. Stroke 37 (10), 2457–2462.

Strbian, D., Tatlisumak, T., Ramadan, U.A., Lindsberg, P.J., 2007. Mast cell blocking reduces brain edema and hematoma volume and improves outcome after experimental intracerebral hemorrhage. J. Cerebral Blood Flow Metabol. 27 (4), 795–802.

Takamatsu, Y., Tamakoshi, K., Waseda, Y., Ishida, K., 2016. Running exercise enhances motor functional recovery with inhibition of dendritic regression in the motor cortex after collagenase-induced intracerebral hemorrhage in rats. Behav. Brain Res. 300, 56–64.

Tang, D.S., Zhang, L., Chen, H.L., Liang, Y.R., Lu, J.L., Liang, H.L., Zheng, X.Q., 2007. Extraction and purification of solanesol from tobacco :(I). Extraction and silica gel column chromatography separation of solanesol. Sep. Purify. Technol. 56 (3), 291–295.

Terai, K., Suzuki, M., Sasamata, M., Miyata, K., 2003. Amount of bleeding and hematoma size in the collagenase-induced intracerebral hemorrhage rat model. Neurochem.l Res. 28 (5), 779–785.

Turner, R.J., Sharp, F.R., 2016. Implications of MMP9 for blood brain barrier disruption and hemorrhagic transformation following ischemic stroke. Front. Cellular Neurosci. 10, 56.

Turunen, M., Peters, J.M., Gonzalez, F.J., Schedin, S., Dallner, G., 2000. Influence of peroxisome proliferator-activated receptor α on ubiquinone biosynthesis. J. Mol. Boil. 297 (3), 607–614.

Wallmark, S., Ronne-Engström, E., Lundström, E., 2014. Prevalence of spasticity after aneurysmal subarachnoid haemorrhage. J. Rehabilit. Med. 46 (1), 23–27.

Wang, J., et al., 2018. Inflammatory cytokines and cells are potential markers for patients with cerebral apoplexy in intensive care unit. Exp. Therapeutic Med. 16 (2), 1014–1020.

Wills, E., 1966. Mechanisms of lipid peroxide formation in animal tissues. Biochem. J. 99 (3), 667.

Wityk, R.J., Caplan, L.R., 1992. Hypertensive intracerebral hemorrhage. Epidemiology and clinical pathology. Neurosurg. Clin. N. Am. 3 (3), 521–532.

Xi, G., Keep, R.F., 2012. Intracerebral hemorrhage: mechanisms and therapies. Transl Stroke Res. 3, 1–3.

Xue, M., Del Bigio, M.R., 2000. Intracerebral injection of autologous whole blood in rats: time course of inflammation and cell death. Neurosci. Lett. 283 (3), 230–232.

Yan, N., Liu, Y., Gong, D., Du, Y., Zhang, H., Zhang, Z., 2015. Solanesol: a review of its resources, derivatives, bioactivities, medicinal applications, and biosynthesis. Phytochem. Rev. 14 (3), 403–417.

Zhang, L., Plotkin, R.C., et al., 2004. Cholinergic augmentation with donepezil enhances recovery in short-term memory and sustained attention after traumatic brain injury1, 2. Arch. Phys. Med. Rehabilit. 85 (7), 1050–1055.

Zhao, J., Bu, Z.W., Liu, Y., 2006. Synthesis and biological activity of new solanesyl nitrogen mustards. Chin. J. Appl. Chem. 23, 514–518.

Zhu, W., Gao, Y., Chang, C.F., Wan, J.R., Zhu, S.S., Wang, J., 2014. Mouse models of intracerebral hemorrhage in ventricle, cortex, and hippocampus by injections of autologous blood or collagenase. PLoS One 9 (5), e97423.